# A Study on Weld Line Morphology and Mechanical Strength of Injection Molded Polystyrene/Poly(methyl methacrylate) Blends

**SHAOYUN GUO,[1] A. AIT-KADI[2]**

[1] The State Key Laboratory of Polymer Materials Engineering and Polymer Research Institute of Sichuan University, Chengdu 610065, China.

[2] CERSIM, Chemical Engineering Department, Laval University, Quebec, Quebec, Canada GIK 7P4

*Received 10 February 2001; accepted 9 June 2001*

**ABSTRACT:** In this work, the mechanical strength and weld line morphology of injection molded polystyrene/poly(methyl methacrylate) (PS/PMMA) blends were investigated by scanning electron microscopy (SEM) and mechanical property test. The experimental results show that the tensile strength of PS/PMMA blends get greatly decreased due to the presence of the weld line. Although the tensile strength without the weld line of PS/PMMA (70/30) is much higher than that of the PS/PMMA (30/70) blend, their tensile strength with weld line shows reversed change. The viscosity ratio of dispersed phase over matrix is a very important parameter for control of weld-line morphology of the immiscible polymer blend. In PS/PMMA (70/30) blend, the PMMA dispersed domains at the core of the weld line are spherically shaped, which is the same as bulk. While in the PS/PMMA (30/70) blend, the viscosity of the dispersed PS phase is lower than that of the PMMA matrix, the PS phase is absent at the weld line, and PS particles are highly oriented parallel to the weld line, which is a stress concentrator. This is why weld line strength of PS/PMMA (30/70) is lower than that of PS/PMMA (70/30) blend. © 2002 Wiley Periodicals, Inc. J Appl Polym Sci 84: 1856–1865, 2002; DOI 10.1002/app.10450

**Key words:** polystyrene; poly(methyl methacrylate); blends; weld line; morphology

## INTRODUCTION

Blending is one of the most economically beneficial routes for developing new polymer materials. For most polymer blends, they are immiscible blends. They are often molded into complicated parts by injection molding, compression molding, and extrusion. In fact, molding of such parts usually produces a weld line once the melt fronts have joined either by impingment flow or around an insert.[1,2] However, the presence of a weld line for molded polymer blends parts have been referred to as the "Achilles heel" of polymer blends. The mechanical strength loss for immiscible polymer blends due to the presence of the weld line is usually much more pronounced than that for their counterparts owing to much more complicated morphology in the weld line region.[3–5] The situation is even more complicated by the presence of orientated domains and minor phase concentration gradients in the weld line region.[6–9] Using compatiblizers to stabilize and reduce minor phase dimensions is found to increase weld line strength.[5,10] The presence of compatibilizer is

*Correspondence to:* Shaoyun Guo (nic7702@scu.edu.cn).

Journal of Applied Polymer Science, Vol. 84, 1856–1865 (2002)

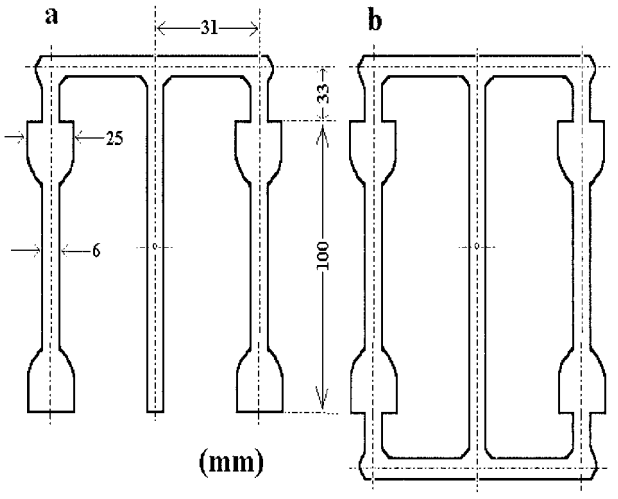


**Figure 1** Schematic diagram of mold cavity used for injection molded samples with and without weld line: (a) no weld line, NWL; (b) with weld line, WL.

also found to narrow the weld line region. The weld line strength could also be improved by selection of suitable injection molding parameters (melt temperature, injection velocity, holding pressure, and mold temperature) to various degrees depending on materials.[11–13] There is no doubt that the increase of weld line strength is finally obtained through development of weld line morphology. So studies on weld line morphology of polymer blends are very profound work.

Despite the fact that weld line morphology of injection molded polymer blends play a very important role in their mechanical strength, only a few studies on this subject has been reported, which does not quite match the growth of polymer blends. Fellahi et al. [10,14] studied the weld line morphology and its stability by addition of compatibilizer in injection molded high density polyethylene/polyamide-6 (HDPE/PA-6) blends. The weld line morphology of HDPE/PA-6 shows three distinct layers: skin, subskin, and core. Scanning electron microscopy (SEM) micrographs show no presence of the minor phase in the skin and weld line. Karger-kocsis et al.[8] studied the morphology–properties relationship and failure behavior of injection molded EPDM toughed PP. The skin/core morphology was found. EPDM phase concentration increases with increasing distance from the skin to the core. The skin shows a thin pure PP layer. The EPDM particles are rich in the core. The presence of the rubber particle concentration gradient was attributed to a faster crystallization of PP in the skin than in the core, which rejects the rubber particles other than surrounding them. However, R. C. Thamn[6] showed different results on studying weld line morphology of injection molded polypropylene (PP)/ethylene propylene diene monomer (EPDM). It was reported that there is lack of dispersed EPDM phase in the weld line region. The viscosity of EPDM has great effects on weld line strength and morphology. Ait-Kadi et al.[4,5] studied the weld line morphology of HDPE/PS/copolymer blends and polycarbonate/polyethylene (PC/PE) (80/20). The results show the presence of dispersed phase in the weld line region. Mielewski et al.[15] identified the cause of weld line weakness in polypropylene systems containing a hindered phenolic antioxidant additive. A combination of techniques—transmission electron microscopy (TEM), Izod impact strength and tensile strength measurements, and x-ray photoelectron spectrometer (XPS)—confirmed that a major cause of weakness in polypropylene weld line was the accumulation of a heater stabilizer additive on the flow front tip and the surface of part. Jarus et al.[16] studied the weld line strength of poly(vinyl chloride) (PVC)/polyethylene (30/70). They ascribed weld line weakness to elongated domains. The elongation of the dispersed phase decreases and weld line strength of the blend goes up as the dispersed phase viscosity is increased above that of the matrix. When the aspect ratio of PVC phase is above 1.24, elongation of the PVC domains led to a brittle weld line.

It can be seen from the reports described above that weld line morphology of polymer blends shows no consistent conclusions. The precise weld

**Table I Zero Shear Viscosity and Flow Activation Energy of PS/PMMA Blends**

| PS/PMMA | 100/0 | 70/30 | 30/70 | 0/100 |
|---|---|---|---|---|
| 180°C | 9.512E5 | 1.371E6 | 3.442E6 | 3.406E6 |
| 200°C | 1.738E5 | 2.425E5 | 5.855E5 | 5.637E5 |
| 220°C | 7.107E4 | 6.803E4 | 1.544E5 | 1.332E5 |
| Ea, kJ/mol | 121.0 | 139.7 | 144.4 | 150.7 |

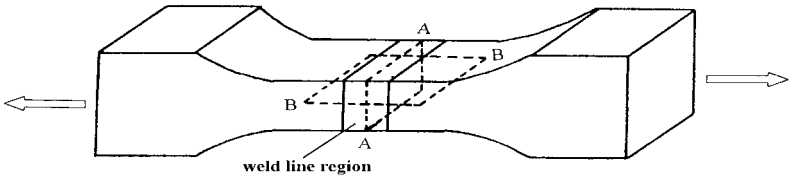


**Figure 2** Schematic diagram of cutting open weld line (A-A: cross section; B-B: longitudinal section).

line profile could not be determined. This information also indicates that weld line morphology of polymer blends may be influenced by many parameters (such as injection temperature, mold temperature, polymer structure, and viscosity ratio of polymer pairs). To the best of our knowledge, there are few reports on the effect of viscosity ratio of the minor phase to the matrix on weld line morphology of polymer blends. In this work, weld line morphology and mechanical strength of PS/PMMA blends as well as effects of viscosity ratio and injection parameters on them were studied. The development of weld line morphology during injection was also discussed.

## EXPERIMENTAL

### Materials

The materials used in this study are PMMA (plexiglas V052, $MI$ = 2.8 g/10 min, $d$ = 1.19 g/cm$^3$, $M_w$ = 55,700) supplied by AtoHass and PS (polystyrene 101, $MI$ = 2.2 g/10 min, $d$ = 1.04 g/cm$^3$, $M_w$ = 295,000) supplied by Novacor Plastics Division.

### Blending

PMMA and PS were dried prior to blending at 78°C for 5 h to remove all the moisture. To investigate the effect of $\eta_d/\eta_m$ (where $\eta_d$ is the viscosity of dispersed phase, $\eta_m$ is the viscosity of matrix) on weld line morphology and strength, two different composition ratios PS/PMMA blends (70/30, 30/70 by weight) were blended in a Haake twin-screw extruder at a screw speed of 60 rpm and a temperature profile ranging from 160°C near the hopper to 200°C at the die exit. The extrudate was then continuously cooled in a water trough and pelletized, then dried.

### Injection Molding

The blends were dried at 80°C for 4 h prior to injection molding. All samples were prepared on a Nissel fully hydraulic 68 tons injection molding machine with a maximum injection capacity of 114 cm$^3$/shot. The mold contained two ASTM

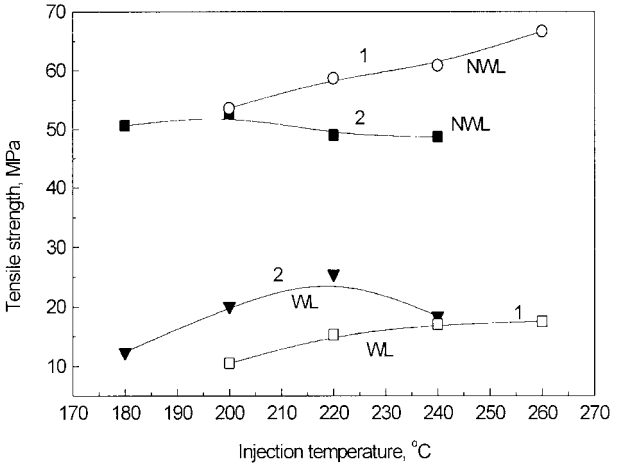


**Figure 3** Effect of injection temperature on tensile strength of PS/PMMA-NWL and PS/PMMA-WL [1: PS/PMMA (70/30); 2: PS/PMMA (30/70)].

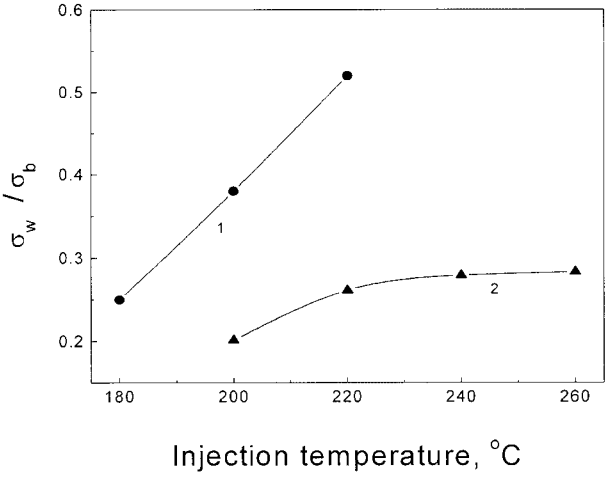


**Figure 4** Effect of injection temperature on $\sigma_w/\sigma_b$ of PS/PMMA [1: PS/PMMA (70/30); 2: PS/PMMA (30/70)].

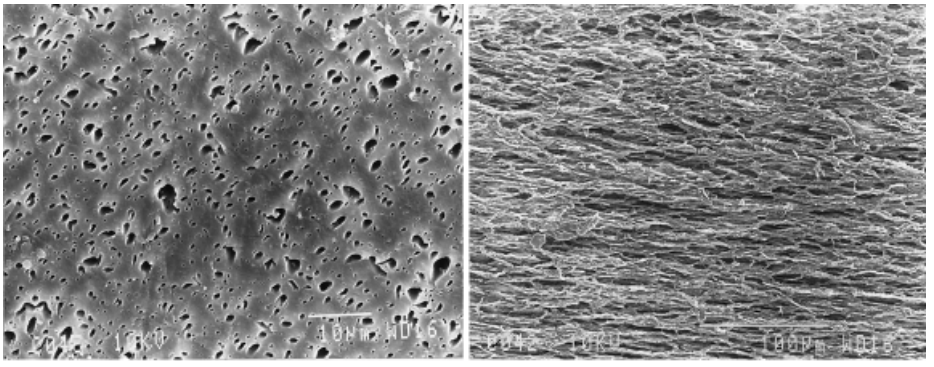

a 70/30, 220℃ b 30/70, 240℃

**Figure 5** SEM photographs of bulk for injection molded PS/PMMA blends.

standard dog bone shaped cavities for mechanical testing for both welded and nonwelded specimens in this study, and is shown in Figure 1. The specimens without a weld line (here called "NWL") and those with weld line called "WL." Injection time is 10 s, cooling time is 25 s, injection temperatures are 180–260°C, and mold temperature is 32°C. Specimens with and without a weld line were prepared.

### Measurement and Characterization

Tensile tests were made using an Instron tensile testing machine at a extension speed of 5 mm/min at room temperature according to the ASTM D638 standard method.

For rheological behavior, the samples were compression molded at 200°C into 25 mm disks in diameter and ca. 1.5 mm in thickness. A Bohlin Rheometer CS was used to measure the dynamic viscoelastic properties of PS, PMMA, and their blends with parallel plate gemotry. Measurements were performed in the frequency range from 0.01 to 10 Hz at temperatures between 180 and 240°C by steps of 20°C. The measurements were done in a nitrogen atmosphere to avoid the thermal degradation of the samples. Strain values were kept with the linear region. The zero viscosity ($\eta_0$) have been determined from Cole–Cole plots of $\eta''$ vs $\eta'$. The activation flow energy of PS, PMMA, and their blends were calculated according to Arrhenius equation $\eta_0 = Ae^{(Ea/RT)}$, where $A$ is a constant, and $Ea$ is the flow activation energy. Table I shows the zero shear viscosity and flow activation energy by dynamic measurements.

For weld line morphology, the tensile fracture surfaces of PS/PMMA blends were covered with a gold–palladium alloy, then observed by a JEOL JSM-840A scanning electron microscope machine. In order to investigate the morphology of the weld line, we cut open the weld line according to the schematic diagram shown in Figure 2 by

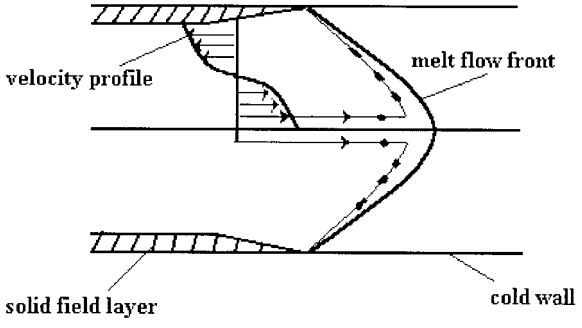


**Figure 6** Schematic diagram of flow pattern in flow front.

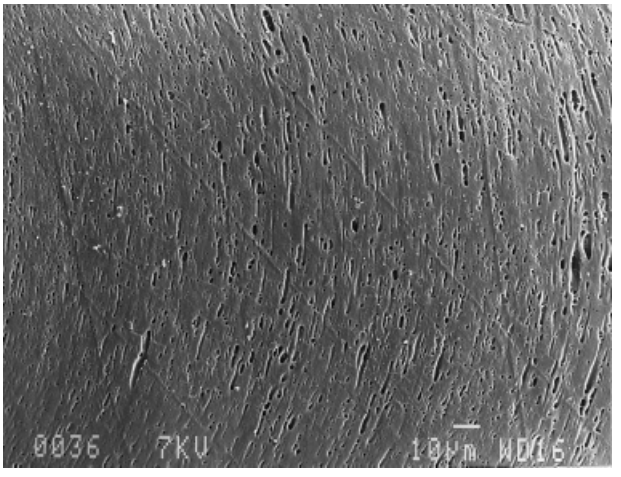


**Figure 7** SEM photograph of flow front of PS/PMMA (70/30) blend.

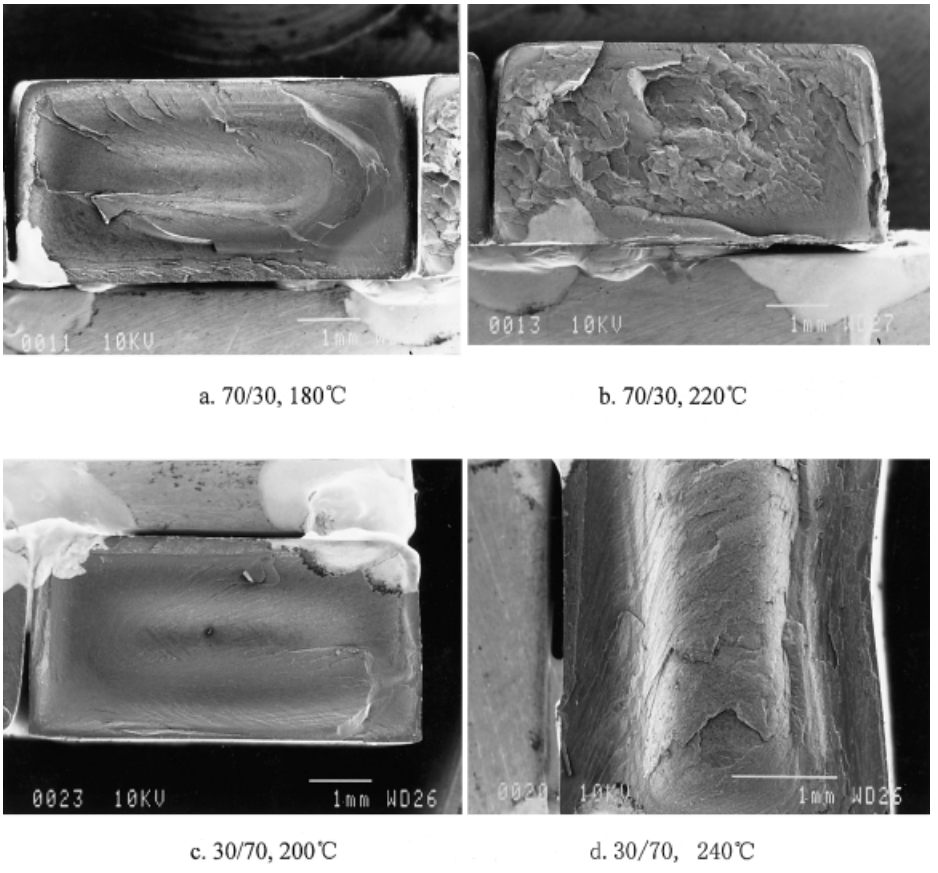


**Figure 8** SEM photographs of tensile fractured surface of injection molded PS/PMMA-WL blends at different injection temperatures.

11–1180 low speed saw apparatus for microstructural analysis (AB Buehler Ltd.). Ethanol was used to cool the saw when the samples were being cut. Then A-A (cross section) and B-B (longitudinal section) sections of samples were polished. The polished samples for PS/PMMA (70/30) were immersed in acetic acid for a period of 24 h at room temperature to dissolve PMMA (dispersed phase). The polished samples for PS/PMMA (30/70) were immersed in carbon tetrachloride for a period of 10 h at room temperature to dissolve the PS (dispersed phase). Following the extraction, the samples were dried in a vacuum oven to remove the solvent. The extracted samples were covered with a gold–palladium alloy and examined in a JEOL JEM-840A scanning electron microscope machine.

## RESULTS AND DISCUSSION

### Mechanical Properties

As shown in Figure 3, tensile strength of PS/PMMA-no weld line (NWL) (70/30) and (30/70) blends shows different change trend with temperature. When the viscosity of dispersed phase is higher than that of the matrix (PMMA as dispersed phase), the tensile strength of the PS/PMMA-NWL (70/30) blend almost stays unchanged as injection temperature rises, which is lower than that of any component in the blend, showing negative derivation from the additivity rule. For the corresponding reverse blend PS/PMMA-NWL (30/70), tensile strength quickly goes up with injection temperature increases. When a weld line was introduced, the fracture of the blend always occurred along the weld line due to its weakness. As shown in Figure 3, although tensile strength of PS/PMMA-NWL (30/70) is higher than that of PS/PMMA-NWL (70/30), the tensile strength of PS/PMMA-with weld line (WL) (30/70) is lower than that of PS/PMMA-WL (70/30). The ratio of WL tensile strength $\sigma_w$ with NWL tensile strength $\sigma_b$ also shows that $\sigma_w/\sigma_b$ of PS/PMMA (30/70) is much lower than that of PS/PMMA (70/30) (Figure 4): The $\sigma_w/\sigma_b$ of PS/PMMA (70/30) is greatly increased with the rise of injec-

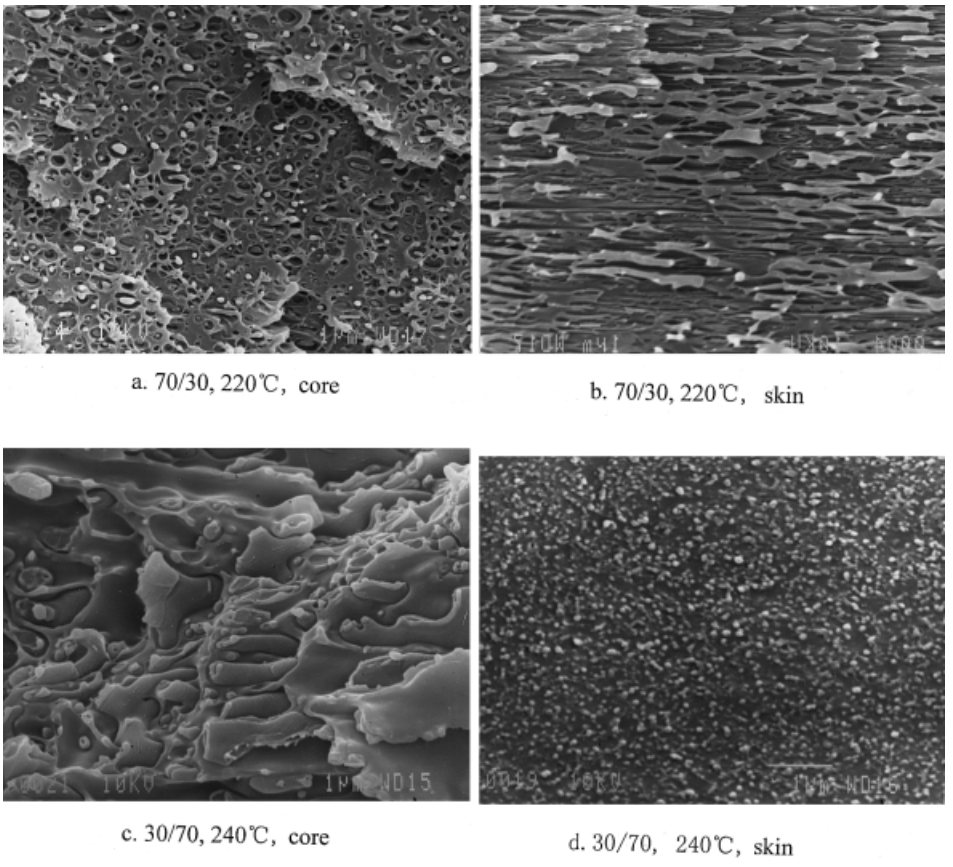


**Figure 9** SEM photographs of skin and core on tensile fractured surface of injection molded PS/PMMA-WL blends.

tion molding temperature, while $\sigma_w/\sigma_b$ of PS/PMMA (30/70) is hardly increased with injection temperature, indicating that $\eta_d/\eta_m$ has great influence on morphology of the blends. This is discussed later.

### Bulk Morphology of the Blends

To observe the bulk morphology of the injection molded parts, we cut open the parts along the injection direction, then polished the section. PS in PS/PMMA (30/70) and PMMA in PS/PMMA (70/30) were dissolved out through carbon tetrachloride and acetic acid respectively. The extracted samples were covered with a gold–palladium alloy and examined in a JEOL JSM-840A scanning electroscope machine. As shown in Figure 5, in the PS/PMMA (70/30) blend, the viscosity of the dispersed PMMA phase is higher than that of the PS matrix during processing temperatures (Table I), the dispersed PMMA domain is hardly deformed during injection, and PMMA domain is a spherically shaped one [Fig. 5(a)]. Therefore, the tensile strength of PS/PMMA-NWL (70/30) slightly changes as the injection temperature rises (Fig. 3). However, the morphology of PS/PMMA (30/70) shows quite a different situation from that of PS/PMMA (70/30). In the PS/PMMA (30/70) blend, the viscosity of the dispersed PS phase is lower than that of PMMA matrix, and PS domain is highly oriented along injection direction [Fig. 5(b)]. The elongation of the PS phase increases as injection temperature rises owing to the decrease of the viscosity of the dispersed PS phase. The oriented PS phase could enhance the tensile strength of the blend. The tensile strength of PS/PMMA-NWL (30/70) increases as injection temperature rises (Fig. 3).

### Weld Line Morphology of Blends

During injection molding, the flow patterns of polymer melts as shown in Figure 6.[17] The flow velocity is decreased from center to wall of the mold. The shear rates, however, shows the opposite tendency: a maximum at the skin and a min-

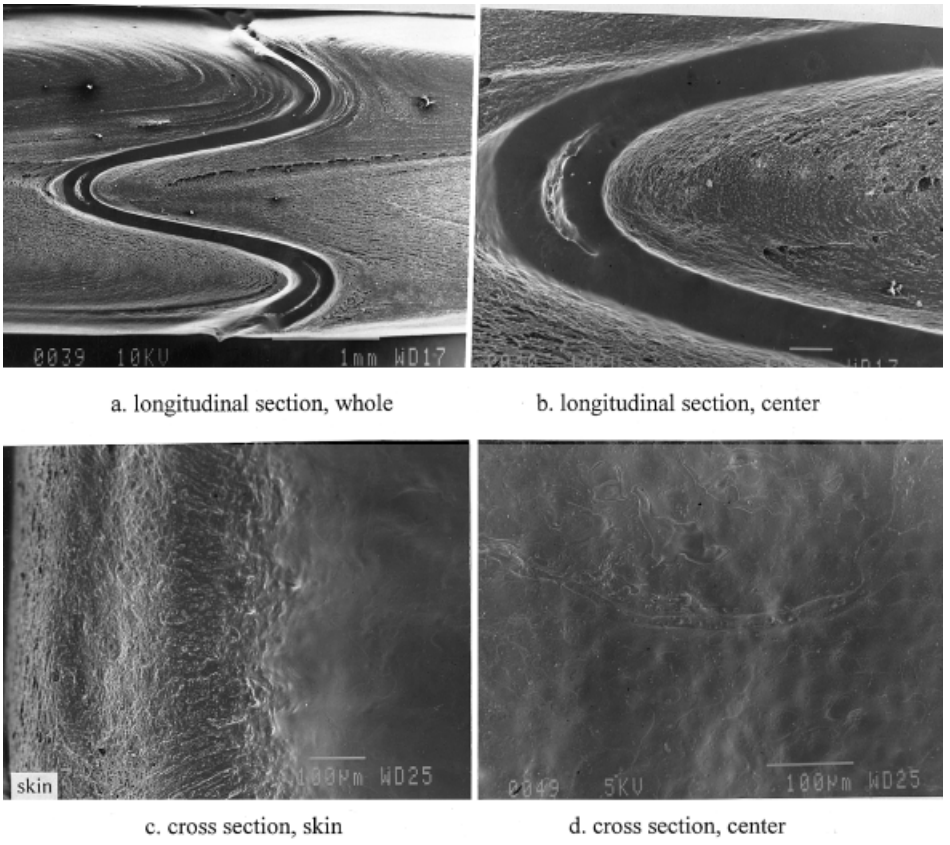


**Figure 10** SEM photographs of cross and longitudinal sections of weld line for PS/PMMA (30/70) (injection temperature: 240°C).

imum at the core. As the fast moving laminar reaches the melt front, flow starts toward the wall and laminar flow changes over to radial flow. Our experimental results also prove this point. As shown in Figure 7, in the melt flow front, the PMMA phase in the PS/PMMA (70/30) blend is oriented along the flow front. When two flow fronts meet together, weld lines are created. For immiscible polymer blends, dispersed domains are usually oriented parallel to the weld line and form minor phase concentration gradients, which causes poor weld line strength of injection molded blends of immiscible polymers. The key for increasing weld line strength is elimination of the oriented domains and dispersed phase concentration gradients at the weld line. The molecular diffusion of polymer blends across the weld line would be advantageous to achieve a strong weld line. So the viscosity of blends and melt flow front temperature will have a great influence on the weld line strength. The temperature profile of the melt flow front shows a maximum at center of the mold and a minimum at the wall during injection. So when two melt flow fronts come together, the molecular interdiffusion at center of mold is easier than at the wall. As shown in Figure 8, the tensile fractured surfaces of PS/PMMA blends with the weld line show visible "sandwich" structure. The core of the fractured surface is rougher than its skin due to easier molecular interdiffusion at the center of mold. The higher the injection temperature is, the rougher the fractured surface is, also indicating the same idea. The tensile fractured surface of PMMA/PS (70/30) are much smoother than that of PMMA/PS (30/70), showing that the viscosity ratio of matrix to dispersed phase has a great influence on the weld line morphology of the blends. Magnified views in Figure 8 show that the spherical PMMA domains at the core of the tensile fractured surface in the PS/PMMA (70/30) blend were indistinguishable from those in the bulk [Figure 9(a)]. PMMA domains at the rim of tensile fractured surface are highly oriented along the weld line [Figure 9(b)]. In the injection molded blend of PS/PMMA (30/70), elongated PS domains perpendicular to ten-

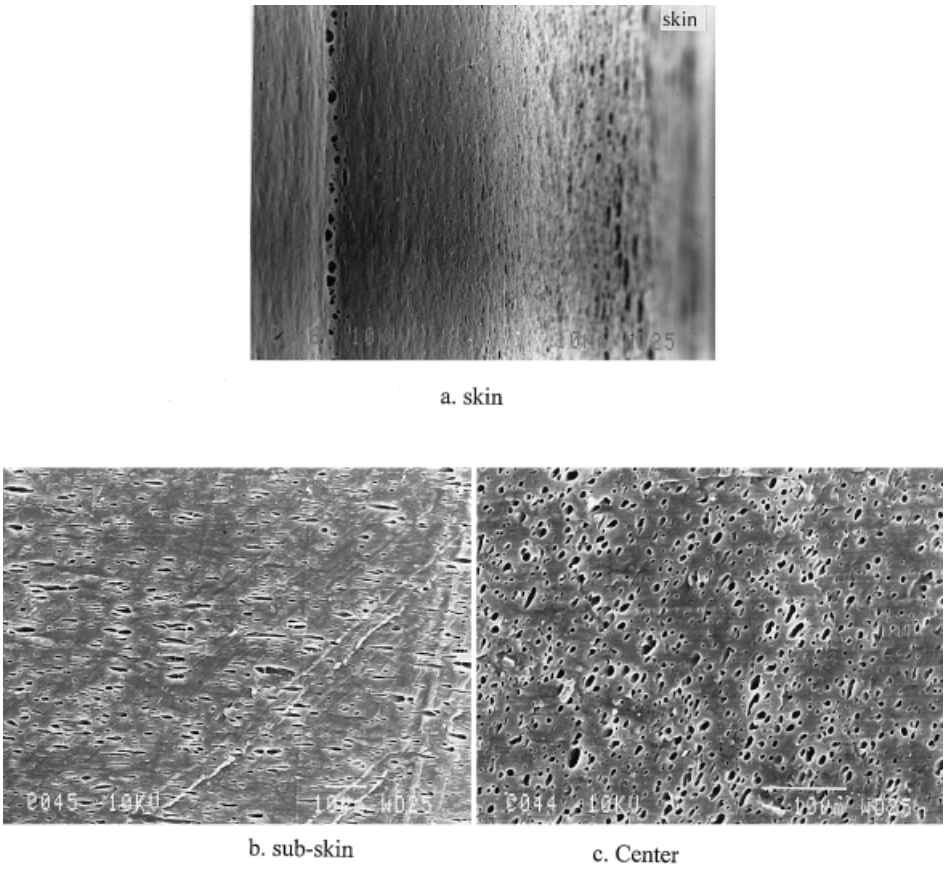


a. skin

b. sub-skin

c. Center

**Figure 11** SEM photographs of cross section of weld line for PS/PMMA (70/30) (injection temperature: 220°C).

sile direction appear at the core of the tensile fractured surface [Figure 9(c)]. The very fine spherical PS domains (0.1 $\mu$m) appear at the rim of the tensile fractured surface of the PS/PMMA (30/70) blend [Figure 9(d)]. In the PS/PMMA (30/70) blend, the viscosity of PS domains is lower than that of the PMMA matrix. PS domains will be deformed under high shear rate at the skin of the weld line during injection. When PS domains are deformed to some extent, highly oriented PS domains will break into smaller particles. So very fine spherical PS domains (0.1 $\mu$m) appear at the rim of the tensile fractured surface of PS/PMMA (30/70) blend.

In order to study the fine morphology of the weld line, we cut open the weld line along the cross section and longitudinal section (Figure 2). Because PS and PMMA are all transparent, while their blends are opaque, so we can observe the weld line morphology of the blend by the naked eye. For the PS/PMMA (30/70) blend, the weld line region is transparent, while for the PS/PMMA (70/30) blend, the weld line region is opaque, indicating the lack of one phase in the weld-line region of the PS/PMMA (30/70) blend. The shape of weld lines has been described as planar or oxbow. In this study, weld line profiles were always oxbow shaped [Fig. 10(a) and Fig. 12(a)]. The thickness (250 $\mu$m) of the weld line in PS/PMMA (30/70) was about 2.5 times the thickness (100 $\mu$m) of the weld line in PS/PMMA (30/70). Figure 10 shows the SEM of cross and longitudinal sections of weld line morphology for the PMMA/PS-WL (70/30) blend (melt temperature 240°C). On the longitudinal section, the weld line appears to consist of escaped and/or deformed PS particles oriented parallel to the weld line [Fig. 10(a)], which is consistent with the SEM of fractured surface [Fig. 9(a)]. But the dispersed PS phase is absent at the weld line [Figure 10(b)]. At the cross section, a rougher surface (500 $\mu$m) is observed at the skin region, attributed to the dispersed PS phase accumulation. However, a shiny sur-

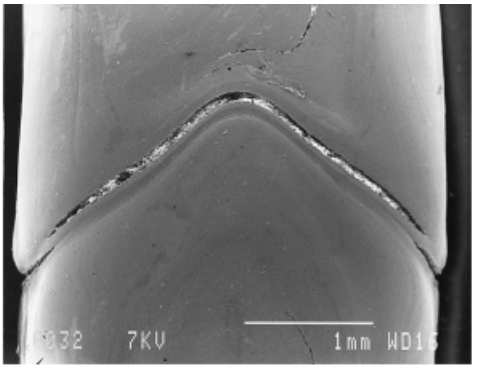


a. whole weld line

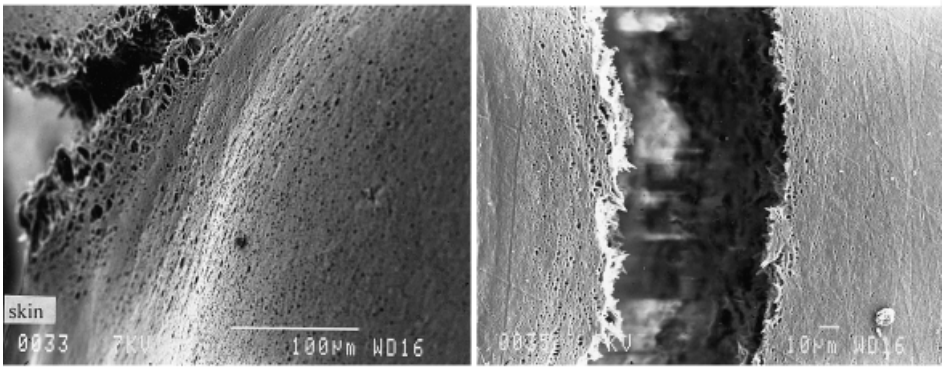


b. skin c. Center

**Figure 12** SEM photographs of lonitudinal section of weld line for PS/PMMA (70/30) (injection temperature: 220°C).

face with smooth topography is observed at the center [Fig. 10(c, d)], also showing lack of dispersed PS phase except skin region.

The morphology of the cross section of the weld line for PS/PMMA (70/30) (Fig. 11) shows that dispersed PMMA in the skin and subskin regions in the weld line region is oriented parallel to the weld line [Fig. 11(a, b)]. The dispersed PMMA phase in the center region of the weld line is an almost spherical particle, which is the same as the morphology of bulk [Figure 11(c)]. As shown in Figure 12, near the weld line, in the skin region, the dispersed PMMA phase in PS/PMMA (70/30) is oriented [Fig. 12(b)] in core region, the dispersed PMMA near the weld line is also spherical shape domain [Fig. 12(c)].

From the above discussion, we can observe that the weld line morphology of PS/PMMA (70/30) is quite different from that of PS/PMMA (30/70). The weld line region of PS/PMMA (70/30) has a rich dispersed PMMA phase, while the weld line region of PS/PMMA (30/70) lacks a dispersed PS phase. This phenomenon may be explained by the following:

The viscosity of PS is lower than that of PMMA (Table I), indicating that PS is more easily deformed by shear than PMMA. In the PS/PMMA (70/30) blend, during two-gate injection molding, when two melt flow fronts meet together, the dispersed PMMA phase could keep the stabilization of the initial spherical droplet shape and migrate to the weld line region during the formation of the weld line. However, when PS is used as the dispersed phase, the situation is quite opposite. In the PS/PMMA (30/70) blend, the dispersed PS phase in the melt flow front deforms more along the front, causing high orientation of PS parallel to melt front. This causes considerable difficulty with interdiffusion as the two melt flow fronts meet together. Moreover, when molecules diffusion goes through the weld line region, the higher viscosity matrix, PMMA, ejects the lower viscosity dispersed PS phase other than surround

it, causing the absence of PS phase at weld line region in PS/PMMA (30/70) blend.

As shown in Figures 3 and 4. The amplitude of the weld line strength increases in the PS/PMMA-WL (70/30) blend is higher than that observed with the PS/PMMA-WL (30/70) blend. This means that weld line morphology is an important parameter on weld line strength variation. The weld line strength is not only attributed to diffusion phenomenon, but also to the orientation effect at weld line. In the PS/PMMA-WL (30/70) blend, there is a lack of the dispersed PS phase at the weld line and the dispersed PS phase near the weld line is highly oriented parallel to the weld line, which is the stress concentrator, causing the decrease of weld line strength.

## CONCLUSIONS

The viscosity ratio of the dispersed phase over a matrix is a very important parameter for control of weld line morphology of an immiscible polymer blend. The weld line morphology of PS/PMMA (70/30) is quite different from that of PS/PMMA (30/70). In the PS/PMMA (30/70) blend, the viscosity of the dispersed PS phase is lower than that of the PMMA matrix, the PS phase is absent at the weld line, and PS particles are highly oriented parallel to the weld line. In the PS/PMMA (70/30) blend, the PMMA dispersed domains at the core of weld line are spherically shaped, which is the same as bulk. Although the $\sigma_b$ of PS/PMMA(70/30) is much lower than that of PS/PMMA(30/70), the $\sigma_w/\sigma_b$ of PS/PMMA(70/30) is much higher than that of PS/PMMA (30/70), which is ascribed to the lack of the dispersed PS phase at the weld line and the high orientation of PS domains parallel to weld line in PS/PMMA (30/70) blend.

The authors are grateful to the Special Funds for Major Basic Research Projects of China (G1999064800), National Natural Science Foundation of China, and the State Education Ministry of China for financial support of this work.

## REFERENCES

1. Fellahi, S.; Meddad, A.; Fisa, B.; Favis, B. D. Adv Polym Technol 1995, 14(3), 169.
2. Bozarth, M. J.; Hamill, J. L. SPE ANTEC Tech Papers 1984, 30, 1091.
3. Nolley, E.; Barlow, J. W.; Paul, D. R. Polym Eng Sci 1980, 20, 364.
4. Mekhilef, N.; Ait-Kadi, A.; Ajji, A. Polymer 1995, 36(10), 2033.
5. Brahimi, B.; Ait-Kadi, A.; Ajji, A. Polym Eng Sci 1994, 34(15), 1202.
6. Thamm, R. C. Rubber Chem Technol 1977, 50, 24.
7. Malguarnera, S. C.; Riggs, D. C. Polym Plast Tech Eng 1981, 17, 193.
8. Karger-Kocsis, J.; Csikai, I. Polym Eng Sci 1987, 27, 241. 1987
9. Fisa, B.; Favis, B. D.; Bourgeois, S. Polym Eng Sci 1990, 30(17), 1051.
10. Fellahi, S.; Favis, B. D.; Fisa, B. Polymer 1996, 37(13), 2615.
11. Kim, S. G.; Suh, N. P. Polym Eng Sci 1986, 26(17), 1200.
12. Titomanlio, G.; Piccarolo, D.; Rallis, A. Polym Eng Sci 1989, 29(1), 4.
13. Kim, S.; Suh, N. P. Polym Eng Sci 1986, 26(1), 17.
14. Fellahi, S.; Fisa, B.; Favis, B. D. J Appl Polym Sci 1995, 57, 1319.
15. Mielewski, D. F.; Bauer, D. R.; Schmitz, P. J.; Van Oene, H. Polym Eng Sci 1998, 38(12), 2020.
16. Jarus, D.; Summers, J. W.; Hiltner, A.; Baer, E. Polymer 2000, 41, 3057.
17. Tadmor, Z. J Appl Polym Sci 1974, 18, 1753.